Research Square

Preprints are preliminary reports that have not undergone peer review.
They should not be considered conclusive, used to inform clinical practice,
or referenced by the media as validated information.

# 316 m of ice beyond the stratified sections of the Beyond EPICA Little Dome C ice core

**Julien Westhoff**

westhoff@nbi.ku.dk

University of Copenhagen

**Lisa Ardoin**

Université Libre de Bruxelles

**Ilka Weikusat**

Ifred-Wegener-Institut Helmholtz-Zentrum für Polar- und Meeresforschung https://orcid.org/0000-0002-3023-6036

**Pierre Henri Blard**

CRPG, UMR 7358, CNRS - Université de Lorraine, France

**Francois Fripiat**

Université Libre de Bruxelles

**Barbara Seth**

University of Bern

**Lison Soussaintjean**

University of Bern

**Manuela Krebs**

Alfred-Wegener-Institut Helmholtz-Zentrum für Polar- und Meeresforschung

**Marie Bouchet**

Niels Bohr Institute

**Ailsa Chung**

Université Grenoble Alpes, CNRS, IRD, IGE

**Federico Scoto**

Ca' Foscari University of Venice, Department of Environmental Sciences, Informatics and Statistics, Via Torino 155, 30172 Venice, Italy https://orcid.org/0000-0003-2498-3227

**Johannes Lemburg**

Alfred-Wegener-Institut Helmholtz-Zentrum für Polar- und Meeresforschung

**Gunther Lawer**

Alfred-Wegener-Institut Helmholtz-Zentrum für Polar- und Meeresforschung

**Matthias Hüther**

Alfred-Wegener-Institut Helmholtz-Zentrum für Polar- und Meeresforschung

**Nicolas Stoll**

Ca'Foscari University of Venice

**Nicholas Rathmann**
University of Copenhagen

**Louise Crinella Morici**
CRPG, UMR 7358, CNRS - Université de Lorraine, France

**Jean-Louis Tison**
Université Libre de Bruxelles

**Olaf Eisen**
Alfred Wegener Institute, Helmholtz Centre for Polar and Marine Research https://orcid.org/0000-0002-6380-962X

**David Lilien**
Indiana University https://orcid.org/0000-0001-8667-8020

**Robert Mulvaney**
Natural Environment Research Council https://orcid.org/0000-0002-5372-8148

**Thomas Stocker**
University of Bern

**Iben Koldtoft**
University of Copenhagen https://orcid.org/0000-0002-5158-1904

**Grant Boeckmann**
University of Copenhagen

**Steffen Hansen**
University of Copenhagen

**Frederic Parrenin**
Université Grenoble Alpes, CNRS, IRD, IGE https://orcid.org/0000-0002-9489-3991

**Frank Pattyn**
Universite libre de Bruxelles https://orcid.org/0000-0003-4805-5636

**Elisabeth Isaksson**
Norwegian Polar Institute

**Margareta Hansson**
Department of Physical Geography, Stockholm University

**Roderik van de Wal**
Utrecht University https://orcid.org/0000-0003-2543-3892

**Hubertus Fischer**
University of Bern https://orcid.org/0000-0002-2787-4221

**Amaelle Landais**
Laboratoire des Sciences du Climat et de l'Environnement https://orcid.org/0000-0002-5620-5465

**Carlo Barbante**
Universita Ca' Foscari Venezia https://orcid.org/0000-0003-4177-2288

**Dorthe Dahl-Jensen**

Center for Ice and Climate https://orcid.org/0000-0002-1474-1948

**Frank Wilhelms**

Alfred Wegner Institute

---

**Article**

**Keywords:**

**Posted Date:** June 11th, 2026

**DOI:** https://doi.org/10.21203/rs.3.rs-9883712/v1

**License:** This work is licensed under a Creative Commons Attribution 4.0 International License.
Read Full License

**Additional Declarations:** There is **NO** Competing Interest.

---

# 316 m of ice beyond the stratified sections of the Beyond EPICA Little Dome C ice core

*Julien Westhoff* (1), Lisa Ardoin (2), Ilka Weikusat (3, 4), Pierre Henri Blard (5, 2), Francois Fripiat (2), Barbara Seth (6), Lison Soussaintjean (6), Manuela Krebs (3, 7), Marie Bouchet (8), Ailsa Chung (9, 6), Federico Scoto (10, 11), Johannes Lemburg (3), Gunther Lawer (3), Matthias Hüther (3), Nicolas Stoll (10, 3), Nicholas Rathmann (1), Louise Crinella Morici (5), Jean-Louis Tison (2), Olaf Eisen (3, 12), David Lilien (13), Robert Mulvaney (14), Thomas F. Stocker (6), Iben Koldtoft (1), Grant Boeckmann (1), Steffen Bo Hansen (1), Frédéric Parrenin (9), Frank Pattyn (2), Elisabeth Isaksson (15), Margareta E. Hansson (16), Roderik van de Wal (17, 18, 19), Hubertus Fischer (6), Amaëlle Landais (8), Carlo Barbante (10), Dorthe Dahl-Jensen (1, 20), & Frank Wilhelms (3, 7)*

**Affiliations**

1 - Niels Bohr Institute, University of Copenhagen, Copenhagen, Denmark
2 - Laboratoire de Glaciologie, Department of Geosciences, Environment and Society, Université Libre de Bruxelles, Brussels, Belgium
3 - Alfred Wegener Institute, Helmholtz Centre for Polar and Marine Research, Bremerhaven, Germany
4 - Department of Geoscience, University of Tübingen, Tübingen, Germany
5 - Centre de Recherches Pétrographiques et Géochimiques, CNRS, Université de Lorraine, 54500, Vandoeuvre Nancy, France
6 - Climate and Environmental Physics, Physics Institute & Oeschger Centre for Climate Change Research, University of Bern, Sidlerstrasse 5, 3012 Bern, Switzerland
7 - University of Göttingen, Geoscience Center, Goldschmidtstrasse 1, D-37077 Göttingen, Germany
8 - Laboratoire des Sciences du Climat et de l'Environnement –CEA-CNRS-UVSQ/IPSL, 91190 Gif sur Yvette, France
9 - Université Grenoble Alpes, CNRS, INRAE, IRD, Grenoble INP, IGE, 38000 Grenoble, France
10 - Ca'Foscari University of Venice, Venice, Italy
11 - Institute of Polar Sciences, National Research Council (ISP-CNR), Venice, Italy
12 - Faculty of Geosciences, University of Bremen, Bremen, Germany
13 - Department of Earth and Atmospheric Sciences, Indiana University, Bloomington, USA
14 - British Antarctic Survey, NERC/UKRI, Cambridge, UK
15 - Norwegian Polar Institute, Tromsø, Norway
16 - Department of Physical Geography, Stockholm University, Sweden

17 - Institute for Marine and Atmospheric Research Utrecht, Utrecht University, Utrecht, the Netherlands
18 - Department of Physical Geography, Utrecht University, Utrecht, the Netherlands
19 - Royal Netherlands Meteorological Institute, de Bilt, the Netherlands
20 - Centre for Earth Observation Science, University of Manitoba, Winnipeg, Canada

# Abstract

At Little Dome C the Beyond EPICA – Oldest Ice project has drilled through the central East Antarctic Ice Sheet to the ice-rock interface at 2,799.85 m depth, recovering the first subglacial rock samples from this region. We describe 316 m of ice composed of four zones, below the well-layered, stratigraphic ice. Just below the stratigraphic ice, we find 22 m of ice, potentially still in stratigraphic order, as DEP-conductivity data and crystal size measurements cannot clearly indicate discontinuities here. Then, in the 77 m-long deformed ice zone, the ice becomes potentially unstratified and deformed, likely folded during flow, and extremely thinned. Below, we find the enigmatic zone, a 212 m-thick zone in which the ice crystals quickly reach multi-centimeter sizes, that appears to reflect prolonged static grain growth under limited deformation. The conductivity signal fluctuates greatly, for which the reason is still unknown. The bottom-most 4.85 m, the debris-rich zone, consists of ice with incorporated silt to fine gravel -sized basal material, mostly within debris-rich bands. Additionally, from the drill chips, we collect angular pebbles between 1-4 mm in diameter. Together, these findings provide the first integrated view of microstructure, rheology, and geology from beneath central East Antarctica, illuminating long-term ice-sheet processes.

# The Beyond EPICA - Oldest Ice project

## Project aims

The European Beyond EPICA - Oldest Ice project has achieved a milestone in palaeoclimatology by drilling through the central East Antarctic Ice Sheet to the ice-rock interface at Little Dome C (LDC) and recovering the first ice core across the Mid Pleistocene Transition (MPT).

Beyond EPICA has two complementary objectives. First, the recovery of well-stratified ice extending beyond 1.2 million years (Ma), providing an unprecedented window into climate dynamics during and before the MPT (~1.2–0.7 Ma) when Earth's glacial cycles shifted from 41,000-year to 100,000-year periodicity, and the mechanisms driving this glacial-interglacial cyclicity. The second objective is the analysis of the debris-rich ice and subglacial sediment samples, just above bedrock, providing insights into ice sheet initiation and pre-glacial ecosystems, basal processes, and the geology of one of Earth's least accessible continental regions. While the stratigraphic ice column is essential for palaeoclimate reconstruction, the debris-rich ice zone might preserve a distinct archive of ice-bedrock interactions, geothermal conditions, and subglacial geology.

The Beyond EPICA drilling achievement provides access to ice potentially older than 1.2 Ma [1]. The potential end of stratigraphic ice lays around 2,484 m depth, and has recovered 316 m of ice beyond that, reaching the interface of ice to subglacial material at 2,799.85 m depth. This extends the continuous ice core climate record deeper into the Early Pleistocene, and possibly beyond the Pleistocene, while the oldest non-continuous ice core reached 6 Ma in the Allan Hills blue ice [2].

Here, we provide a first characterisation of the physical properties of the lower-most 316 m, which extend beyond the stratigraphic ice section. We also provide the first results from a comprehensive analysis of ice-rock interface processes from central East Antarctica.

## Site overview and basal temperature

During the site selection survey [3], a site was chosen that does not have basal melting, i.e., temperatures well below the pressure melting point at the bottom of the ice sheet, the ice-rock interface [4] (and Mulvaney/Ritz et al., in prep.). The LDC drilling site (75°06'S, 123°21'E) is situated 35 km south-east of the EPICA Dome C (EDC) site along the present-day ice flow trajectory [1, 5]. Ice thickness at LDC reaches approximately 2,800 m, 460 m shallower than EDC (3,260 m) [6]. This reduced ice thickness ensures that no basal melting occurs at this site, i.e. melting away layers from the bottom of t which is a prerequisite to finding ice covering the MPT [7].

The exact temperature at the ice-rock interface can only be measured in the borehole and is difficult to model. Then, this temperature can be used to determine the geothermal heatflux.

The annual surface temperature at EDC is -54.5 °C [8] and borehole temperature measurements at various depths suggest bottom temperature to be around -8 °C (see methods). This provides a first estimate for the geothermal heat flux of 51 ± 5 [mW/m2].

## Stratigraphic Observations

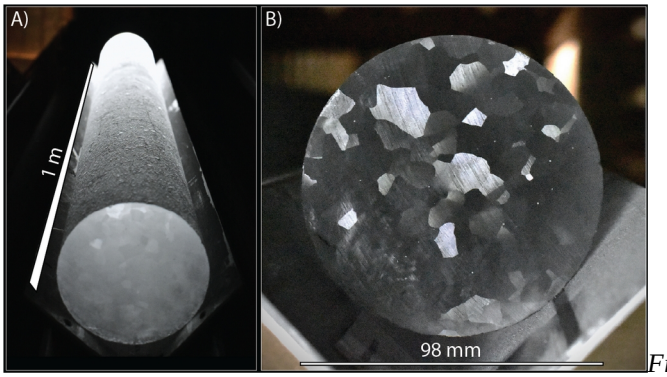



*Figure 1: Bag 2633 in the backlight illumination setup. A) the ice core is being illuminated from top to bottom and B) shows the resulting optical appearance of the individual crystals.*

For the first time, using various on-site techniques in combination, we were able to distinguish different zones of the ice core prior to its shipment out of Antarctica. We deploy a novel and simple technique to analyse changes in crystal texture, such as size and shape, with depth in the field, with measurements up to every meter. This method is based on diffused light of a flashlight, centered behind the ice core and a camera imaging the bag-cut plane of the ice core (Fig. 1, see also methods section). Additionally, we use dielectric profiling (DEP) [9] to measure the electrical conductivity in the ice core, which among other variations indicates volcanic events serving as chronology markers and also provides a proxy for climate system processes.

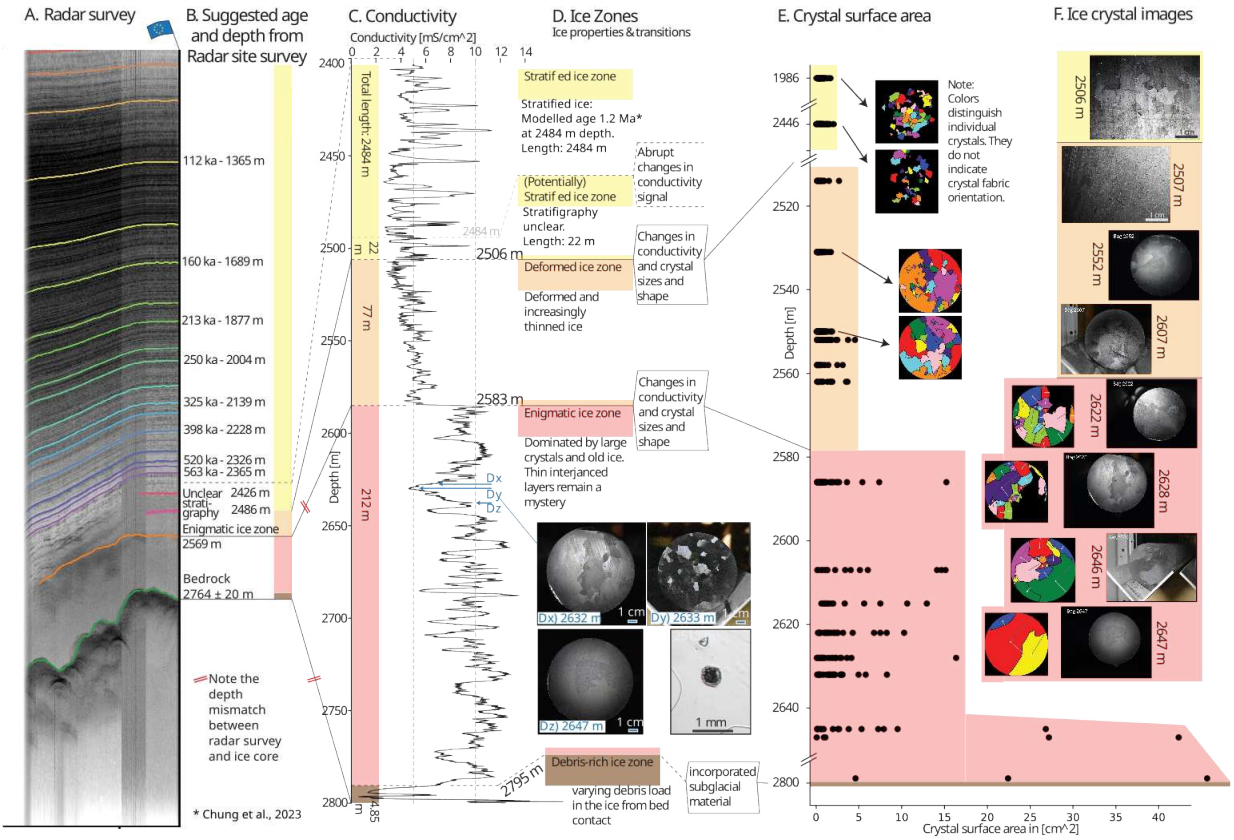



*Figure 2: Radar survey from the site selection campaign, drill site selected at the flag (A), with age and depth estimates of the corresponding isochrones (B). Conductivity profile from 2400 to 2800m depth (C) and the division into stratified, deformed, enigmatic, and debris-rich ice zones (D). Measurements of crystal sizes against depth (E) from images shown in (F). False colour images in (E) and (F) represent individual crystals, not crystal orientation.*

## The stratified ice zone (0 m to 2506 m)

To a depth of 2506 m, the ice core likely consists of stratified, well-layered ice. As a preliminary interpretation, the DEP signal appears to follow climatic cycles [10], and visual inspections imply that crystal sizes remain relatively small, below 2.5 $cm^2$ (Fig. 2). The age predicted by a 1D model [11] reaches 1.2 Ma at 2484 m and 1.5 Ma at 2506 m. In this section from 2484 m to 2506 m, no final stratigraphy can be determined from the field measurements to date. A more detailed examination of the potentially stratigraphic zone, 2484-2506 m, is currently underway but beyond the scope of this paper.

## The deformed ice zone (2506 m to 2583 m)

The top of the deformed zone, i.e., at 2506 m depth, marks a significant shift across all analysed parameters (Fig. 2C,E,F and methods section). The changes of DEP and crystal patterns could imply that the ice core record below may likely be disturbed, potentially by folding, and a stratigraphic order does not exist anymore. Hence, we refer to these 77 m as the deformed ice zone.

### The enigmatic ice zone (2583 m to 2795 m)

Crystal size increases rapidly from 2583 m depth, and by ~2650 m, approximately 150 m above bedrock, individual 10 cm-cut sections of the core often contain fewer than two distinct crystals (e.g. Fig. 2Dz, 2647 m). Throughout the enigmatic ice zone, multi-centimeter, sometimes greater than 10 cm in diameter, crystals are visible on the exterior of the ice cores (Fig. S1_2). The conductivity signal suddenly increases to a higher baseline at 2583 m (Fig. 2C), which persists over the next 212 m, with great fluctuations. Whether these fluctuations are a climatic signal remains unknown to date. Yet, at 2633 m, crystal size abruptly becomes smaller with individual crystals being more interlocked, similar to ice from the stratified section of the core (Fig. 2Dy). Throughout the enigmatic ice section, and occasionally above, we find mineral aggregates (Fig. 2D) with a diameter of 0.5 to 1 mm. These aggregates resemble those found by [12] in the bottom tens of meters of the Dome C ice core.

## Stratigraphic interpretation

Within the conductivity data (Fig. 2C) at the bottom of the stratified ice zone, we observe abrupt signal changes, which, without additional measurements and age information, appear to be too sudden to result from climatic transitions. Potential candidates for the end of stratigraphic ice are at depths of 2484 m, 2488 m, 2499 m, and 2506 m, within the 22 m of the potentially stratified zone, Fig. 2C. One of these transitions marks the end of the stratigraphic ice. Which one precisely is yet to be determined. While an earlier depth could mark the end of the stratigraphic zone, the transition at 2506 m coincides with changes in crystal texture, which we therefore interpret as the boundary between stratified and deformed ice. The reduced amplitude of the conductivity signal in the deformed ice could potentially align with the older sections of the marine sediment core stack, e.g. the Pliocene [10], indicating old ice and possibly a large stratigraphic hiatus at the transition at 2506 m. On the other hand, the more stable conductivity signal in the deformed ice zone could indicate rearrangement of the impurities and a first step to crystal size increase, while the deformed possibly mixes Glacials and Interglacials, thus flattening the signal.

The transition from the deformed into the enigmatic ice zone (at 2583 m depth, Fig. 2) is again marked by a jump in DEP-derived conductivity values and a substantial increase in crystal size, suggesting the presence of an additional stratigraphic hiatus.

In modeling studies (e.g. [11]), estimating the age of stratigraphic ice at the Beyond EPICA drill site, the more than 200 m section of enigmatic ice is often treated as non-deforming on present-day velocity scales, i.e., stagnant, with vertical deformation rates rather similar to the base in comparison to the stratified ice above. In these bottom 200+ m, we observe large crystals, suggesting prolonged normal or static grain growth without the effects of strain-induced grain-size reduction. The ice appears stagnant today, for most practical aspects, but crystal and conductivity data hint at either remnants of stratified layers within the enigmatic ice zone or active individual shear planes reducing crystal size. Both effects could be the result of large-scale folding. One such instance of smaller crystals is at 2633 m depth, which warrants a detailed future study.

Consequently, the term stagnant should be considered as a relative term with respect to the deformation rates of the ice above the enigmatic ice unit. The origin of this ice still remains a mystery. It could be similar to the claim for the Gamburtsev mountains [13], where refrozen water originated from the top of the table mountain. Yet this would induce different crystal sizes and a drop in conductivity, neither of which was observed. The opposite is observed, as large crystals hint to very old ice, due to long crystal growth periods and higher conductivity values hint to ice from warmer periods, e.g. the early Pleistocene, Pliocene, or even older.

## Subglacial samples from the debris-rich ice zone (2795 m to 2799.85 m)

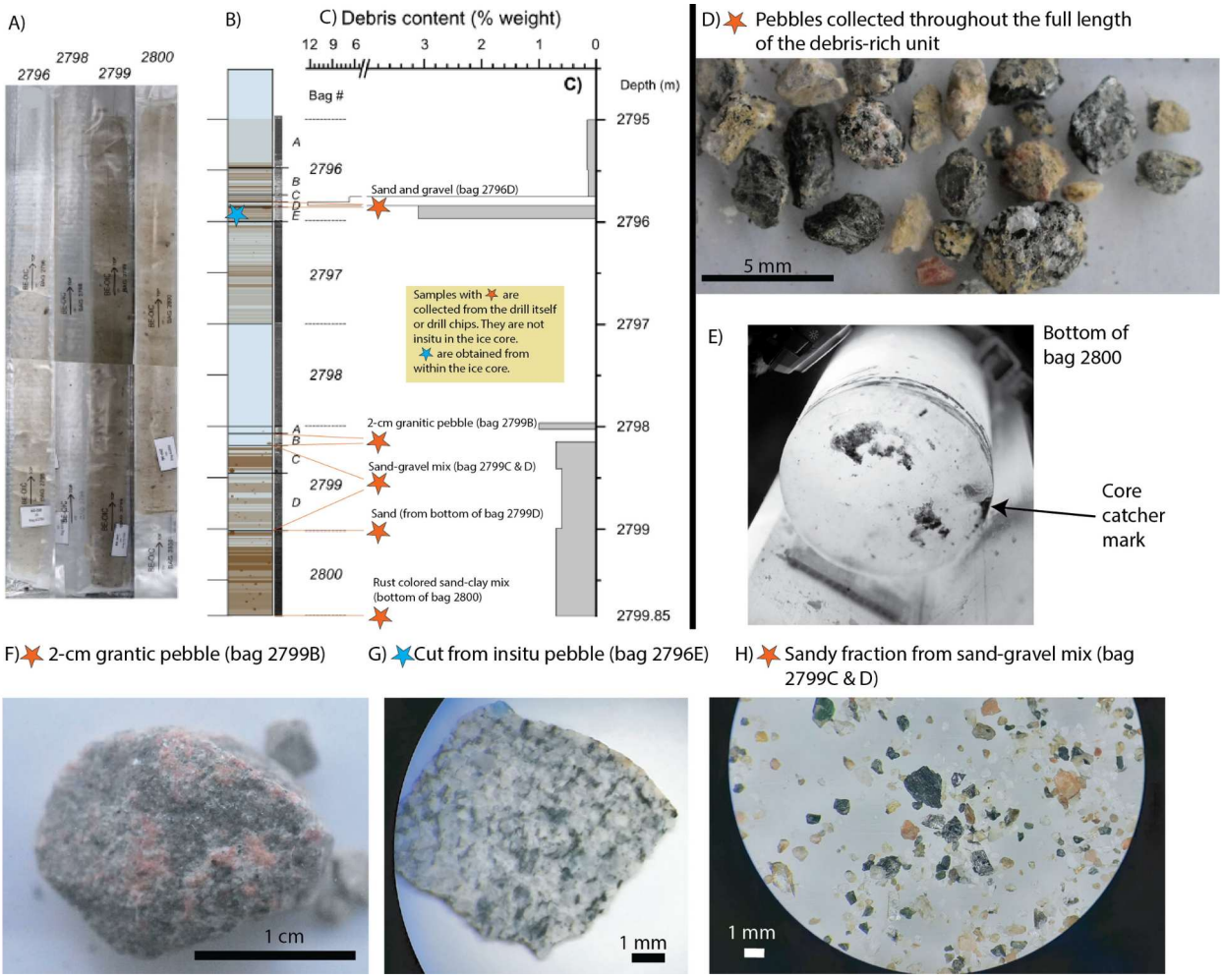



*Figure 3: The bottom-most 4.85 m of the ice core (2795–2799.85 m). A) Four of the five cut sections (7 cm width) with bag numbers. B) Stratigraphic column of the debris-rich ice; blue is ice with a very low debris-load, visible but not measurable, and the darker the brown, the higher the debris-load. C) Debris content (wt%) versus depth as averages between core breaks. Bag 2796D without gray shading due to measurement difficulties. D) Rock samples collected from drill chips. The majority of them have a granitic composition. E) Bottom of the Beyond EPICA LDC ice core at 2799.85 m depth. F) granitic sample from the drill chips and G) granitic sample from inside the ice core. H) Sand section of bag 2799C and D under a microscope.*

The first appearance of basal geological debris occurs at a core break at 2795 m, where sand-sized and smaller particles are embedded within the ice matrix, along with occasional centimetre-scale pebbles. The debris-rich section displays heterogeneous content with colour variations associated

with debris content changes (Fig. 3). Following the facies classification of [14], the intervals 2795.0-2797.0 m and 2798.2-2799.85 m correspond to a banded dispersed facies, featuring debris-rich layers thicker than 1 mm and debris content up to 12 wt% (Fig. 3C and methods section). In contrast, the interval 2797.0 m and 2798.2 m shows a clean facies (<1 wt% debris), lacking visible layering and containing occasional frozen-in debris with a diameter < 1 cm.

## Rock Samples

During the drilling process, we also recovered several rock fragments (Fig. 3, orange stars) from the drill chips, which were originally set in the debris-rich ice. They reached the surface by bypassing the drill head via the chip transport-spirals (clearance 3-4 mm), into the chip's chamber of the drill. Most of them range in size from 1–5 mm, and are thus coarse sand to fine gravel (size definition [15]).

From visual inspection (Fig. S1_4 to S1_23), these rock fragments have angular to subangular shapes, while they have various petrological natures. The large majority of these rock fragments are of an igneous granitic origin, but from different rock source types: these fragments indeed display variable silica contents: granitic lithologies (quartz, felspars, biotites) are the most abundant fragments, while Fe-Mg-rich rock (probably pyroxenes or amphiboles) is also present in significant proportion. Some granitic fragments are coated with a yellowish clay alteration layer, firmly adhering to the surface. Further mineralogical (XRD, SEM and thin sections analysis) and geochemistry (REE, Rb/Sr, Sm/Nd) work is underway to refine these characterisations.

## Ice-rock contact (2799.85 m)

Core number 2800 (2799.00 to 2799.85 m) marks the deepest ice core retrieved to date (Fig. 3E). Further penetration has not been possible with the ice or rock drills.

The bottom surface of this core shows clear indications of rock contact:

- Visible debris adhered to the surface indicates an ice-rock interface.
- A smooth, unbroken interface, suggesting no additional ice directly beneath.
- The mark of the core catcher (Fig. 3E) shows no signs of wedging and breaking, and the core break strength was too low for breaking ice.
- The ice drill cutters resurfaced severely damaged, implying contact with rock not drillable with the ice core drill. It cannot be distinguished whether this damage is caused by one rock, a rock layer, or bedrock.

## Subglacial interpretation

The 4.85 m of debris-rich ice exhibits a facies and a debris content that look similar to that observed in Greenland [16, 17, 18, 19, 20] and elsewhere in Antarctica [21, 22]. In these sections, debris incorporation may occur either through mechanical mixing processes at the ice–bed interface, such as shearing and folding [18, 23], or through the freezing of subglacial meltwater at the base of the ice sheet [21, 22]. Additional measurements such as gas content and water isotopic composition are required to distinguish between these mechanisms [24, 22].

Debris-rich ice from Greenlandic cores has preserved biological signatures of microbial activity that potentially predate the formation of the ice sheet or are evidence of subglacial biological activity [25, 26, 27, 28, 29, 17]. Whether similar biosignatures are present in the debris-rich basal ice of the BELDC core remains to be investigated by upcoming measurements on gases, potential fossil remains, and organic molecules.

Collecting rocks from beneath a nearly 3 km-thick Antarctic ice sheet is exceptionally rare. We recovered granitic rocks of at least two different lithologies. This hints at subglacial processes mixing lithologies from different origins. The yellowish clay alteration layer (Fig. 3D, S1_11 & S1_16) suggests the presence of water for its formation. This alteration is either the result of pedogenesis during previous ice free conditions or the impact of subglacial hydrological processes. With not all rocks being coated with an  alteration layer, further processes of transportation in liquid water must also have occurred sometimes in between. Today, the very slow surface velocity at LDC (50 mm/yr, [1]), the presence of a large-crystal in the 212 m thick enigmatic ice unit, and temperatures of -8 °C do not indicate strong sliding at the ice-rock interface, as well as no liquid water. Under these cold conditions, where no basal water is present, ice flow is accommodated by internal deformation, mostly confined to the ice above 2583 m rather than basal sliding (Mulvaney/Ritz et al., in prep.). The rocks collected from (the outside of the drill and) drill chips have a strong grain size bias to 1-4 mm, due to internal drill clearances (see methods). They are angular to sub-angular suggesting erosion with negligible water present. Rocks inside the ice core (in-situ rocks) range in grain size from clay or silt to gravel, suggesting the presence of a wider granulometric population at the ice-rock interface. Further investigations such as SEM analysis of the grain textures and characterisation of the clays assemblages will permit a better characterization of the debris history before and after their incorporation in the ice.

# Conclusion & Outlook

The drilling of the Beyond EPICA core was highly successful. Ice believed to contain some of the oldest stratigraphically preserved records ever drilled is found at a depth of around 2428 m (age: approx. 800 ka b2k). At 2484 m, we find stratified ice with a preliminary age that reaches the target of 1.2 Myr [1] and potentially more stratigraphic ice until to 2506 m depth. This leaves 316 m of ice for investigation below that.

The deformed ice (2506 m to 2583 m), and potentially even the enigmatic ice, represent a new opportunity to study climatic periods older than the MPT, albeit possibly without a continuous record. Further studies are needed to determine if and how this ice can be used for palaeoclimatic studies.

Furthermore, the 212 m of enigmatic ice—due to its extremely large crystals—could be mechanically more resistant to deformation, which is the working-hypothesis for depth-age scale in current (ice age-) models [11]. This could result in ice deformation being primarily accommodated above 2583 m, creating a distinct interface between the stratified and deformed ice column above and the enigmatic ice below. Yet, the interspersed layers of smaller crystals remain a mystery, as they hint to dynamics within this unit. Thus the deformed and enigmatic ice zones remain interesting to investigate physical properties of ice and ice rheology, as well as palaeoclimatic signals.

The collected rock samples suggest the, or at least “a”, ice–rock interface to be just below the current borehole bottom (2799.85 m). In everyday language in the ice core community, any rock that can not be penetrated with the ice core drill will be referred to as bedrock. Real bedrock may be deeper, and a layer of glacial till with incorporated ground-down granite (as found in this study) may lay on top, which would be referred to as a sedimentary layer. To further refine the subglacial stratigraphy we would now need to deploy a rock drill, which has not recovered core so far (see methods).

In this study, we have defined the bottom sections of the Beyond EPCIA ice core using terminology that removes ambiguities across different ice core communities. We also present the first results, mainly from the field, to distinguish these zones. The newly developed method of on-site crystal size determination excels in simplicity and practicality. Analysis of the debris-rich ice gives first insights into the subglacial environment and opens the door to many further studies.

# References


[1] Chung, A. et al. Age, thinning and spatial origin of the Beyond EPICA ice from a 2.5D ice flow model, *The Cryosphere*, **19**, 4125–4140, https://doi.org/10.5194/tc-19-4125-2025 (2025).

[2] Shackleton, S. et al. Miocene and Pliocene ice and air from the Allan Hills blue ice area, East Antarctica, *Proc. Natl. Acad. Sci. U.S.A.*, **122**, 44, https://doi.org/10.1073/pnas.2502681122 (2025).

[3] Lilien, D. A. et al. Brief communication: New radar constraints support presence of ice older than 1.5 Myr at Little Dome C, *The Cryosphere*, **15**, 1881–1888, https://doi.org/10.5194/tc-15-1881-2021 (2021).

[4] Van Liefferinge, B. et al. Promising Oldest Ice sites in East Antarctica based on thermodynamical modelling, *The Cryosphere*, **12**, 2773–2787, https://doi.org/10.5194/tc-12-2773-2018 (2018).

[5] Parrenin, F. et al. Is there 1.5-million-year-old ice near Dome C, Antarctica?, *The Cryosphere*, **11**, 2427–2437, https://doi.org/10.5194/tc-11-2427-2017 (2017).

[6] Tison, J.-L., et al. Retrieving the paleoclimatic signal from the deeper part of the EPICA Dome C ice core, The Cryosphere, 9, 1633–1648, https://doi.org/10.5194/tc-9-1633-2015 (2015).

[7] Fischer, H., et al. Where to find 1.5 million yr old ice for the IPICS "Oldest-Ice" ice core, Climate of the Past, **9**, 2489–2505, https://doi.org/10.5194/cp-9-2489-2013 (2013).

[8] EPICA community members. Eight glacial cycles from an Antarctic ice core, Nature, **429**, 623–628, https://doi.org/10.1038/nature02599 (2004).

[9] Wilhelms F, Kipfstuhl J, Miller H, Heinloth K, & Firestone J. Precise dielectric profiling of ice cores: a new device with improved guarding and its theory. *Journal of Glaciology*, **44,** 146, 171-174, https://doi.org/10.3189/S002214300000246X (1998).

[10] Ahn, S., Khider, D., Lisiecki, L. E., & Lawrence, C. E. A probabilistic Pliocene–Pleistocene stack of benthic δ18O using a profile hidden Markov model, *Dynamics and Statistics of the Climate System*, **2**, 1, https://doi.org/10.1093/climsys/dzx002 (2017).

[11] Chung, A. et al. Stagnant ice and age modelling in the Dome C region, Antarctica, *The Cryosphere*, **17**, 3461–3483, https://doi.org/10.5194/tc-17-3461-2023 (2023).

[12] de Angelis, M., Tison, J.-L., Morel-Fourcade, M.-C., & Susini, J. Micro-investigation of EPICA Dome C bottom ice: evidence of long term in situ processes involving acid–salt interactions, mineral dust, and organic matter, *Quaternary Science Reviews*, **78**, 248-265, ISSN 0277-3791, https://doi.org/10.1016/j.quascirev.2013.08.012 (2013).

[13] Bell, R. et al. Widespread Persistent Thickening of the East Antarctic Ice Sheet by Freezing from the Base, Science, **331**, 1592-1595. https://doi.org/10.1126/science.1200109 (2011).

[14] Hubbard, B., Cook, S., & Coulson, H. Basal ice facies: a review and unifying approach, *Quaternary Science Reviews*, **28**, 19–20, 1956-1969, https://doi.org/10.1016/j.quascirev.2009.03.005 (2009).

[15] ISO 14688-1:2017, Geotechnical investigation and testing — Identification and classification of soil — Part 1: Identification and description (2017).

[16] Bender, M., Burgess, E., Alley, R.B., Barnett, B., & Clow, G.D. On the nature of the dirty ice at the bottom of the GISP2 ice core, *Earth and Planetary Science Letters*, **299**, 3–4, 466-473, https://doi.org/10.1016/j.epsl.2010.09.033 (2010).

[17] Verbeke V., Lorrain R., Johnsen S.J., & Tison J.-L. A multiple-step deformation history of basal ice from the Dye 3 (Greenland) core: new insights from the CO2 and CH4 content. *Annals of Glaciology*, **35**, 231-236, https://doi.org/doi:10.3189/172756402781817248 (2002).

[18] Tison, J.-L., Thorsteinsson, T., Lorrain, R.D., & Kipfstuhl, J. Origin and development of textures and fabrics in basal ice at Summit, Central Greenland, *Earth and Planetary Science Letters*, **125**, 1–4, 421-437, https://doi.org/10.1016/0012-821X(94)90230-5 (1994).

[19] Goossens, T., Sapart, C. J., Dahl-Jensen, D., Popp, T., El Amri, S., and Tison, J.-L.: A comprehensive interpretation of the NEEM basal ice build-up using a multi-parametric approach, The Cryosphere, **10**, 553–567, https://doi.org/10.5194/tc-10-553-2016 2016.

[20] Herron, S. L. formerly Hoar, S. L. & Langway, C. C. jr. The Debris-Laden Ice at the Bottom of the Greenland Ice Sheet, *Journal of Glaciology*, **23**, 89, 193-207, https://doi.org/doi:10.3189/S002214300002983X (1979).

[21] Gow, A.J., Epstein, S., & Sheehy, W. On the Origin of Stratified Debris in Ice Cores from the Bottom of the Antarctic Ice Sheet, *Journal of Glaciology*, **23,** 89, 185-192, https://doi.org/10.3189/S0022143000029828 (1979).

[22] Gow, A.J. & Meese, D. Physical properties, crystalline textures and c-axis fabrics of the Siple Dome (Antarctica) ice core. *Journal of Glaciology*.**53** (183), 573-584, https://doi.org/10.3189/002214307784409252 (2007).

[23] Souchez R.A. & Jouzel J. On the Isotopic Composition in δD and δ18O of Water and Ice During Freezing, Journal of Glaciology, **30**, 106, 369-372, https://doi.org/10.3189/S0022143000006249 1984.

[24] Souchez, R. et al. Gas isotopes in ice reveal a vegetated central Greenland during ice sheet invasion, *Geophys. Res. Lett.*, **33**, L24503, https://doi.org/10.1029/2006GL028424 (2006).

[25] Christ, A.J. et al.-A multimillion-year-old record of Greenland vegetation and glacial history preserved in sediment beneath 1.4 km of ice at Camp Century, *Proc. Natl. Acad. Sci. U.S.A.*, **118,** 13, e2021442118, https://doi.org/10.1073/pnas.2021442118 (2021).

[26] Christ, A.J. et al. Deglaciation of northwestern Greenland during Marine Isotope Stage 11, *Science*, **381**, 330-335, https://doi.org/10.1126/science.ade4248 (2023).

[27] Willerslev, E. et al. Ancient Biomolecules from Deep Ice Cores Reveal a Forested Southern Greenland. *Science*, **317**, 111-114, https://doi.org/10.1126/science.1141758 (2007).

[28] Souchez, R., J.Jouzel, A.Landais, J.Chappellaz, R.Lorrain, & J.-L.Tison , Gas isotopes in ice reveal a vegetated central Greenland during ice sheet invasion, Geophys. Res. Lett., **33**, L24503, https://doi.org/10.1029/2006GL028424 (2006).

[29] Miteva, V.I., Sheridan, P.P., & Brenchley, J.E. Phylogenetic and Physiological Diversity of Microorganisms Isolated from a Deep Greenland Glacier Ice Core. *Appl Environ Microbiol*, **70**, https://doi.org/10.1128/AEM.70.1.202-213.2004 (2004).

# Methods

## Basal temperature and geothermal heatflux

The annual surface temperature at EPICA Dome C (EDC) is -54.5 °C [M1], and the same values can be applied to LDC. By measuring the borehole temperature in different depths we extrapolated the bottom temperature to be around -8 °C.

We measured borehole temperatures in a simplistic field approach. We used an industrial temperature logger from Lascar Electronics (EL-USB-1-PRO high temperature data logger), mounted in a pressure and liquid-tight aluminum housing, with a coupling to the top of the inner core barrel of the ice drill. This reduces the maximum ice core length by approx. 20 cm, but enables simultaneous temperature logging and ice core drilling.

The logger is limited to -40 °C, limiting exact measurements on the way, as annual average temperatures range around -54.5 °C. We measured -21.4 °C at 2200 m, -16.8 °C at 2400 m, and -12.4 °C at 2600 m during production drilling. Linear interpolation suggests a temperature of approximately -7.9 °C at 2800 m depth.

This provides a first guess of the geothermal heat flux, using

$\Phi q = -K*dt/dz = (2.27*(17-8)/(2800-2400) = 51$ [mW/m2].

Including the measurement uncertainty, the heat flux is 51 ± 5 [mW/m2].

## Radio-echo sounding

The radargram in Fig.2A was collected with a ground-based VHF radar in 2019. Standard, unfocused SAR processing was applied. Layers were traced semi-automatically, following amplitude peaks. The peaks were dated using the point of closest approach to the EDC core site and transferred from the AICC2012 age scale to AICC2023. Details of the system, processing, and interpretation can be found in [M2].

## Dielectric profiling

We used the dielectrip profiling (DEP) device developed at Alfred Wegener Institute, Germany (AWI, [M3]). Two opposing electrodes travel along the ice core, measuring the electrical conductivity and permittivity every millimeter. We measured the entire ice core to obtain this high resolution profile. The signal provides indications of volcanic eruptions to match the ice core to other known profiles and it provides a proxy for a climatic record, revealing climatic warm and cold cycles in the signal.

## Backlight core illumination for crystal size and texture

### Measurement setup

We use a standard camping flashlight (Kathmandu Ruru, 300 Lumen), modified with a cone and diffusive milky paper the size of the ice core. This ensures even illumination behind the core (Fig. 1). The cone and a 3D-printed holder center the light source behind the ice core while it rests in aluminum trays for two days before core processing. Ambient temperatures range between –35 °C and –45 °C, depending on activity in the facility.

We position a DSLR camera (Nikon D7200) with a Nikkor 40 mm macro lens roughly centered in front of the ice core. The camera's position is varied slightly to increase the number of visible crystals, and multiple images are taken with small angular adjustments around the 90° axis to the ice core cutting plane (Fig. 1).

We use Adobe Illustrator to stack the images and manually trace the crystal boundaries. Using images taken under varying illumination conditions enhances the number of visible crystal reflections. We then export the binary crystal boundary network as a PNG file.

We re-purposed a Python-based image analysis pipeline for processing large-area scanning microscope (LASM) images of ice core thin/thick sections. The code uses established computer vision and scientific computing libraries (e.g., scipy, scikit-image, OpenCV (cv2), matplotlib, pandas, and PyQt5 for GUI interaction) to perform image preprocessing, segmentation, and quantitative feature extraction, contrasting traditional pixel-based analysis with modular scripting for automated, reproducible workflows. It extracts the following parameters: grain count, x/y coordinates, equivalent diameter, true area, eccentricity, orientation, perimeter, and the lengths of major and minor axes.

### Limitations of optical in-field crystal measurements

The method of using in-field crystal measurements has some limitations. We rely exclusively on cuts where the basal planes of crystals are oriented to refract light toward the camera setup. These likely represent grains aligned as a single-maximum fabric. In other fabric configurations, grains may not be visible, leading to potential underrepresentation of the number of grains. In samples from the stratified and deformed zones, the high number of grains and indistinct crystal boundaries can cause an overestimation of grain size. Crystals with the same orientation next to each other are easy to measure as one. In contrast, within the enigmatic ice zone, crystals exceed the core diameter, making them immeasurable in full, and therefore, only a minimum grain size estimate can be provided. The issue of missing grain boundaries will be addressed using laboratory-based techniques, such as the LASM [M4].

Despite these limitations, the optical in-field method has proven to be highly effective, requiring minimal additional effort and providing real-time analysis of transitions in ice properties. This

information is valuable for rheological properties of the ice and the whole Physical Properties community, but also for logistics planning, particularly for ensuring the safe transport of the most scientifically valuable ice sections.

## Naming convention of the enigmatic ice zone

The bottom 217 m, i.e. the enigmatic and debris-rich ice zones—sometimes also referred to as stagnant ice in the modeling community [M5] or as the basal unit in the radar community [M2]—is well known across Antarctica from radar surveys [M6, M7] and from other deep ice cores [M8, M9]. These 217 m are treated as one unit in the modelling and radar communities, due to lack of resolution near the ice sheet bottom. The ice at the ice-bed interface contains debris and is referred to as basal ice in the geology and subglacial processes communities [M8]. To remove this naming confusion, we suggest the term enigmatic ice zone for the bottom 212 m and debris-rich ice zone for the bottom 4.85 m of ice, avoiding naming ambiguities.

## Recovering and sampling debris-rich ice

### Debris-rich ice drilling and dark core handling

A noticeable drop in drill performance due to the presence of rocks marked the transition to dark ice core handling procedures. Upon surfacing, the drill exited directly into a ~2 m long black tube (nicknamed the “Wurst”) made of layered paper and plastic bags. This sealed the bottom of the core barrel from light exposure.

The Wurst was folded and tied shut using a rope setup to ensure complete light-tightness. The top part of the core barrel was also covered using a paper bag system. The entire barrel was carried into the underground facility at LDC for core extraction under red-light conditions, using headlamps (Black Diamond, Spot) set to red. Four operators used one lamp each during handling and no additional light was in the room.

With cleaning paper, we removed as much drill fluid from the outside as possible. Then, we sectioned the core using a standard wood-cutting handsaw, where necessary, and processed according to the standard ice core logging procedure [M10]. Final depth corrections based on remeasured sections placed the ice-rock interface at 2799.85 m, adjusting for a previously introduced 2 cm offset. The field report can be found in supplement 2.

## Recovering basal rocks from the drill chips and the ice core drill

During debris-rich ice drilling, we recovered numerous rock fragments from both the ice core drill and the drill chips. Rock fragments with a shorter axis <4 mm can travel through the helical flights between the inner and outer core barrels, ending up in the drill's chip chamber.

After drill chip recovery, we carefully searched the slush in a drip pan, collecting rock fragments using tweezers (Fig. 3, orange stars). These rocks were exposed to daylight and are therefore unsuitable for optically stimulated luminescence (OSL) dating, but they provided valuable information for the petrological identification of the basal lithology.

Collected samples were examined first with a 10× magnifying lens and later re-evaluated via high-resolution imagery (Fig. S1_9). Identification was based on visual inspection of mineral content, grain structure, and colour.

## Attempts on further penetration

After using the ice drill during the 2024/2025 drilling season, the Danish/Swiss rock drill was deployed, but operational difficulties (e.g., thread unwinding) hindered recovery. The drill head became firmly lodged in the borehole's center. After high-load retrieval, no bedrock core was recovered, and further drilling attempts were suspended until the next season.

In the 2025/26 drilling season, five runs recovered material from the bottom of the borehole with the rock drill (Supplement 3). Four of these consisted of refrozen water, probably originating from the drill heating the surrounding ice during rotation. The fifth core contained a 3 cm-thick layer of rock fragments (similar to Fig. 3D) locked in a matrix of refrozen water. As of today, the deepest core of non-altered ice was drilled using the ice drill in January 2025 (in the 2024/2025 drilling season, Fig. 3E).

## Dark Procedure in the Ice Core Lab at AWI, Europe

At the AWI ice core laboratory (Germany), under red light conditions, we estimated debris content by weighing the core segments and measuring their volume. Hereby, we assume an ice density of 0.9167 g/cm³ and a rock density of 2.7 g/cm³. The uncertainties associated with debris content are relatively large, primarily due to the irregular shape of the core. This irregularity can cause a nugget effect, particularly in smaller samples such as pieces 2796C and -D (covering approximately 2795.7 to 2795.8 m). The clean facies section contains <1 wt% debris, which could not be detected by our debris content measurement method, yet is visible by eye.

# Method references


[M1] EPICA community members. Eight glacial cycles from an Antarctic ice core, Nature, **429**, 623–628, https://doi.org/10.1038/nature02599 (2004).

[M2] Lilien, D. A. et al. Brief communication: New radar constraints support presence of ice older than 1.5 Myr at Little Dome C, The Cryosphere, 15, 1881–1888, https://doi.org/10.5194/tc-15-1881-2021 (2021).

[M3] Wilhelms, F., Kipfstuhl, J., Miller, H., Heinloth, K., & Firestone, J. Precise dielectric profiling of ice cores: a new device with improved guarding and its theory. Journal of Glaciology, 44, 146, 171-174, https://doi.org/10.3189/S002214300000246X (1998).

[M4] Krischke, A., Oechsner, U. and Kipfstuhl, S. Rapid Microstructure Analysis of Polar Ice Cores. Optik & Photonik, 10, 32-35, https://doi.org/10.1002/opph.201500016 (2015).

[M5] Chung, A. et al. Stagnant ice and age modelling in the Dome C region, Antarctica, The Cryosphere, 17, 3461–3483, https://doi.org/10.5194/tc-17-3461-2023 (2023).

[M6] Young, D. A. et al. Coupled Ice Sheet Structure and Bedrock Geology in the Deep Interior of East Antarctica: Results From Dome A and the South Pole Basin, Geophysical Research Letters, 52, e2025GL115729, https://doi.org/10.1029/2025GL115729 (2025).

[M7] Eisen, O. Inferring Antarctic ice dynamics and boundary conditions from the ice sheet's basal unit. GeophysicalResearch Letters, 52, e2025GL120048. https://doi.org/10.1029/2025GL120048 (2025).

[M8] Tison, J.-L., et al. Retrieving the paleoclimatic signal from the deeper part of the EPICA Dome C ice core, The Cryosphere, 9, 1633–1648, https://doi.org/10.5194/tc-9-1633-2015 (2015).

[M9] Crotti, I. et al. An extension of the TALDICE ice core age scale reaching back to MIS 10.1, Quaternary Science Reviews, 266, 107078, https://doi.org/10.1016/j.quascirev.2021.107078 (2021).

[M10] Hvidberg, C.S., Steffensen, J.P., Clausen, H.B., Shoji, H., & Kipfstuhl, J. The NorthGRIP ice-core logging procedure: description and evaluation, Annals of Glaciology, 35, 5-8, https://doi.org/10.3189/172756402781817293 (2002).

## Acknowledgements

This publication was generated in the frame of Beyond EPICA. The project has received funding from the European Union's Horizon 2020 research and innovation programme under grant agreement No. 815384 (Oldest Ice Core). It is supported by national partners and funding agencies in Belgium, Denmark, France (Grant-No. CNRS/INSU/F2G), Germany (Grant-No. AWI_ANT_30), Italy (Grant-No. PNRA16_00124), Norway, Sweden, Switzerland (Grant-No. 20FI21_189533), The Netherlands and the United Kingdom. Logistic support is mainly provided by PNRA and IPEV through the Concordia Station system. The opinions expressed and arguments employed herein do not necessarily reflect the official views of the European Union funding agency or other national funding bodies. This is Beyond EPICA publication number XX (adjust XX when manuscript is accepted).


## Author contributions

***JW**- conceptualized the manuscript and wrote most sections, development and implementation of the crystal measurement method, initial analysis of debris-rich ice. **LA** - logging, documentation, and analysis of debris-rich ice. **IW** - support on creating the crystal measurement setup. **IW**, **NS,** **JW** - crystal analysis and context. **PHB**, **FF**, **JLT** - analysis of debris-rich ice. **JW**, **LS**, **MK**, **MB**, **FS**, **IK**, **AC** - acquisition and logging of ice core. **AC**, **FP**, **DL** - interpretation from flow models to the ice core. **JL**, **GL**, **MH**, **BS** - acquisition of ice core and discussions on ice-rock interface. **BS**, **JW** - acquisition and sample collection of pebbles. **NR** - crystal analysis tool development and implementation. **LCM** - in-depth analysis of the debris-rich ice. **OE**, **DL**, **RM** - radar survey and depth isochrones context. **GB**, **SBH** - technical implementation to acquire the ice core. **TFS, FP, EI, MEH, RvdW, HF**, **AL**, **CB**, **DDJ**, **FW** - results in perspective, **DDJ** - borehole temperature data and implications, **FW** - DEP data and interpretation, **All** - all authors read, commented, and agree to the manuscript.*

## Competing interests

The authors confirm that there are no competing interests.

## Data/code availability

Code availability for crystal detection software: https://github.com/nicholasmr/LASM

## Materials and correspondence


Correspondence to: Julien Westhoff, University of Copenhagen, Denmark, westhoff@nbi.ku.dk

## Supplementary Files

This is a list of supplementary files associated with this preprint. Click to download.

- BeyondStratigraphy20260531suppl2.pdf
- BeyondStratigraphy20260531suppl3.pdf
- BeyondStratigraphy20260531suppl1.pdf